Environmental Science
Processes & Impacts

Study on spatial and temporal distributions of contaminants emitted by Chinese New Year' Eve celebrations in Wuhan

Journal:	*Environmental Science: Processes & Impacts*
Manuscript ID:	EM-ART-11-2013-000588.R2
Article Type:	Paper
Date Submitted by the Author:	21-Dec-2013

Complete List of Authors:	Han, Ge; Wuhan University, State Key Laboratory of Information Engineering in Surveying, Mapping and Remote Sensing Gong, Wei; Wuhan University, State Key Laboratory of Information Engineering in Surveying, Mapping and Remote Sensing Quan, Jihong; Hubei Environmental Monitoring Central Station, Li, Jun; Wuhan University, State Key Laboratory of Information Engineering in Surveying, Mapping and Remote Sensing Zhang, Miao; Wuhan University, State Key Laboratory of Information Engineering in Surveying, Mapping and Remote Sensing

Burning of firecrackers on the Chinese New Year's Eve(NYE) is an ancient cultural tradition in China. However, such activities deteriorate ambient air quality seriously. This study is aiming at revealing the spatial and temporal distributions of contaminants due to the NYE celebrations. The scale and degree of such influences are much larger than people thought. We hope this study help both governments and people in China reflect on unrestrainedly burning of firecrackers on the NYE. A balance between folk custom and human health is urgent and indispensable.

Journal Name

RSCPublishing

ARTICLE

Spatial and Temporal Distributions of Contaminants Emitted because of Chinese New Year's Eve Celebrations in Wuhan

Cite this: DOI: 10.1039/xoxxoooooox

Received ooth January 2012,
Accepted ooth January 2012

DOI: 10.1039/xoxxoooooox

www.rsc.org/

Ge. Han,[a] Wei. Gong,[a] J.H. Quan,[b] Jun. Li,[a] and Miao. Zhang[a]

Abstract: Activities involving firecrackers and fireworks on the Chinese New Year's Eve (NYE) are common in Chinese culture. Previous studies revealed that such human activities significantly influence the ambient air quality and negatively impact human health. However, both the academia and the public lack a deep understanding of the extent and consequences of such human-induced air pollution. Therefore, it is important to evaluate the effects of these Spring Festival celebrations on ambient air quality at a large spatial scale and a fine temporal resolution. Data from ten monitoring stations distributed around Wuhan and a Lidar system provide a good opportunity to gain insight into spatial and temporal distribution of contaminants due to the NYE celebrations. Dramatic increases in $PM_{2.5}$ and PM_{10} mass concentrations due to NYE celebrations were observed in this study. Moreover, the ratio of residential to total area was found to be a significant factor in predicting the geographic distributions of contaminants. The vertical distribution of such human-induced and culture-related contaminants was first shown using a Mie Lidar. Contaminants emitted by firecrackers on the ground spread to a distance of over 450 m in the atmosphere. The vertical influence began to fade two hours after celebrations because of dry deposition. Moreover, it took over 15 hours for the contaminant levels to return to pre-celebration levels. Finally, estimations of $PM_{2.5}$ emissions from firecrackers in Wuhan were 39.57 and 43.51 tons, based on regression and time series analyses, respectively.

Introduction

In many countries around the world, people celebrate special days with fireworks. The Chinese New Year is a particularly popular event that is celebrated with firecrackers. Almost every Chinese family ignites firecrackers on New Year's Eve (NYE). In most cities in China during 1993-2006, there was a ban on the manufacture, sale, and use of fireworks and firecrackers aimed at reducing the risk of fire. In consideration of cultural traditions and infrastructure development, the ban was lifted in 2007. Recently, however, dense fog and haze enveloped most parts of northern, central, and eastern China, raising new concerns over ambient air quality. Burning fireworks generate contaminants, such as sulphur dioxide, carbon monoxide, nitrogen oxide, suspended particles, and metals such as potassium, aluminium, and manganese, which significantly deteriorate air quality, induce changes in both lung and heart function[1-3], and cause serious health problems[4, 5]. Hence, a better understanding of the distribution and transport of such human-induced contaminations may help the society to achieve a balance between ambient air quality and cultural traditions.

Tiwari found that PM_{10} (particulate matter with an aerodynamic diameter smaller than, or equal to, 10 μm) rose to 723 μg/m^3 from an average of 114μg/m^3 because of an extreme usage of fireworks (during the Diwali festival) in Delhi[6]. Ambient air $PM_{2.5}$ (particulate matter with an aerodynamic diameter smaller than, or equal to, 2.5 μm) also reportedly rose in Lucknow city owing to fireworks during Diwali festival[7]. Rao [8] and Sarkar [9] conducted a chemical analysis of $PM_{2.5}$ and PM_{10} samples collected during Diwali celebrations. Using 24-h data collected over 8 weeks at two sites in Girona, Spain, Moreno reported the effect of a major firework event on urban background atmospheric $PM_{2.5}$ chemistry[10]. Samples collected during Las Fallas in Valencia were also reported[11]. Physical properties, including elements, ions, organic and elemental carbon, and particle size distributions of airborne particles collected during a fireworks episode in Milan (Italy) were reported, and the element strontium (Sr) was recognized as the best fireworks tracer[12]. The chemical composition and chemically resolved

size distributions of fine aerosol particles were measured at a high time resolution (5 min) using a time-of-flight aerosol mass spectrometer (TOF-AMS) during the New Year's 2005 fireworks in Mainz, central Germany[13]. Tsai studied the influences of fireworks on chemical characteristics of fine and coarse atmospheric particles in Kaohsiung City through field measurements of atmospheric particulate matter conducted during the Chinese Lantern Festival[14]. Chang[15] and Wang[16] have also reported air quality changes due to fireworks during the Lantern Festival. The effects of Lantern Festival fireworks on the air quality in Beijing was first assessed on the basis of the ambient concentrations of various air pollutants[17]. Zhang studied the concentration and size distribution of contaminant particles due to firework displays during Chinese New Year in Shanghai[18]. Feng collected seventeen $PM_{2.5}$ samples during the Chinese New Year holiday in Shanghai to determine the composition and sources of fine particles[19].

In summary, previous studies have thoroughly discussed how fireworks and firecrackers influence concentrations and chemical compositions of particulate matter and gaseous pollutants. However, sparse monitoring stations and shortcomings of existing observational techniques constrained research on the spatial and temporal distribution of pollutants emitted by burning firecrackers and fireworks. Besides, activities involving fireworks and firecrackers on Chinese NYE are spontaneous, intensive, and widely distributed, in contrast to other such celebrations around the world. Moreover, such activities, appearing annually in all Chinese cities, significantly impact billions of people. Therefore, there is an urgent need to explore how such large-scale human activities affect ambient air quality.

With the assistance from Hubei Environmental Monitoring Central Station (HEMCS), we collected hourly mass concentrations of $PM_{2.5}$, PM_{10}, and gaseous pollutants including sulphur dioxide, nitric oxide, nitrogen dioxide, carbon monoxide, and ozone from 10 sites distributed around the city of Wuhan during NYE, starting from the last day of the Chinese Lunar Calendar. We examined the citywide influence of simultaneous firecracker burning on ambient air quality on an accurate temporal scale and extensive spatial scale to enhance both the academia's and the ordinary citizen's knowledge about the effect of human customs and culture on the atmospheric environment. Moreover, a Mie Lidar[20] located in Wuhan University was used to probe aerosol extinction coefficients 150–15000 m above ground, providing the first information on the vertical distribution of contaminants emitted from firecrackers. On that basis, we applied time series and regression analyses to estimate $PM_{2.5}$ emissions from NYE celebrations.

Methodology

Measurement sites

Wuhan, located at the intersection of the Yangtze and Han rivers, is the capital of the Hubei province and the political, economic, financial, cultural, educational, and transportation centre of central China. It consists of three towns: Wuchang, Hankou, and Hanyang, facing each other across the two rivers. The metropolis extends over 8,494 km^2 (developed area is 500 km^2) with a population of 8 million (http://www.whbgt.gov.cn/documents.php?c=1&list=new).

Hourly mass concentrations of PM_{10} and $PM_{2.5}$ were measured from 10 air quality monitoring stations distributed around Wuhan. The station names were: Wuchangziyang, Hanyangyuehu, Donghuliyuan, Hankoujiangtan, Hankouhuaqiao, Wujiashan, Donghugaoxin, Zhuankouxinqu, and Chenhuqihao, abbreviated as WC, HY, DH, JT, HQ, WJ, GX, ZK, and CH, respectively. The time resolution of the original data was one hour. We collected data from these sites for February 2013.

Station WC faced a park and is a few kilometres away from a big railway station located in Wuchang district, which is famous as an education centre. HY was located at the foot of Gui mountain in Hanyang district, which was once China's primary industrial hub. JT is situated near Yangtse river in Hankou district; the most famous business centre in central China. HQ and QS are located in residential areas for native Chinese, while GX is located in a newly developed residential area inhabited by many immigrants. WJ is located in a newly developed area where inhabitants have recently transformed from peasants to urban dwellers. DH is located in a park near the East Lake.

CH is situated 50 km southwest of the urban area. Sporadic rural housing is still found 2 km away from this site, according to high-resolution satellite imagery. Though this site is affected by firecracker activities, their influence is negligible compared to that in other sites. Hence, the CH site can be regarded as a control site to evaluate the influence of urban firecracker activities, although this site is not absolutely free of firecracker activity.

ZK is located in an industrial zone where production activity was suspended during the Chinese New Year holiday, and the nearest residential area is about 2 km away. This site was also used as a control site upon considering the temporal resolution of our data, which was one hour, and the diffusion velocity of contaminants released by fireworks and firecrackers. The distribution of these sites is illustrated in Figure 1. Meteorological data were also collected at all sites. The details of technologies adopted in the sampling and analysis are described in the national standards of PR China[21]. Data descriptions are shown in Table 1. The measuring methods of meteorological data are presented in the corresponding national standards.

Figure 1. Distribution of monitoring stations

Table 1. Data Descriptions

observation	detection limit	unit	measuring method
PM10	1μg/m^3	μg/m^3	TEOM
PM2.5	1μg/m^3	μg/m^3	TEOM
wind speed	0.1m/s	m/s	QX/T 51-2007[22]
wind direction	1°	degrees	QX/T 51-2007
temperature	0.1℃	degree celsius	QX/T 50-2007[23]
relative humidity	1%	percents	QX/T 50-2007
atmospheric pressure	0.1hPa	Pascal	QX/T 49-2007[24]

Lidar

Lidar is a powerful active tool for detecting the optical properties of atmospheric aerosols. Vallar[25] and Calhoun[26] utilized Lidar to monitor plumes due to fireworks display. A Lidar ceilometer was used to observe a plume emanating from a pyrotechnic display of 30-min duration[27]. This is the first time atmospheric aerosol optical properties were measured during citywide firework and firecracker activities. Firecrackers burn primarily on the ground, whereas firecrackers burn in air. On NYE, firecrackers played a dominant role in celebrations, so the vertical atmospheric structure data could differ from those of other countries. Our Lidar system consisted of three parts: a laser, telescope optical receiver, and signal acquisition recorder. Detailed specifications are listed in Table 2. The Lidar system was based on a double frequency Nd:YAG laser at 532 nm. The Mie backscatters at 532 nm and the nitrogen Raman backscatters at 607 nm were collected by a Schmidt Cassegrain telescope and separated by dichroic mirrors. A semi-custom bandpass filter and a standard bandpass filter were used in Mie channels. The Raman data was not used in this study, so only Mie Lidar parameters are presented. Our Lidar was installed on the roof of the State Key Laboratory of Information Engineering in Surveying Mapping and Remote Sensing (LIEMARS). The nearest residential area is less than 300 m away.

Table 2. Specification Parameters of Mie Lidar

Transmitter: Nd:YAG Laser	
Wavelength:	532 nm
Pulse Energy:	200 mJ
Pulse Repetition Rate:	10 Hz
Pulse Width:	~ 8ns
Receiver: Schmidt Cassegrain Telescope	
Optical Diameter:	356 mm
Focal Length:	3556 mm
Detector: PMT	Hamamatsu 7400
Mie Channel:	
CWL:	532 nm
FWHM:	5±1 nm
Out-of-Band Rejection:	$<10^{-4}$
Minimum Transmission:	50%
Data Acquisition:	
Analog Acquisition:	12 bit,20MHz
Photon Counting:	250MHz

Results and discussion

Variation of Particulate Matter Mass Concentrations

In 2010, Global Burden of Disease (GBD) indicated ambient particulate matter ranked fourth among all risk factors for deaths in China[28]. Dramatic worldwide increases in atmospheric particulate matter concentrations due to fireworks displays were found. Our $PM_{2.5}$ and PM_{10} data reveal influences of firecrackers on ambient air quality in Wuhan.

In the original data obtained at the ten sites, the PM_{10} concentration was usually lower than the $PM_{2.5}$ concentration. According to our investigation, there was a drying process in weighing measurement for both $PM_{2.5}$ and PM_{10}; however, a humidity compensation device is adopted only for $PM_{2.5}$ measurement because $PM_{2.5}$ was measured by new equipment which is following a stricter standard, revised in 2012. During this period, the mean relative humidity was 77%, so on most days the measured $PM_{2.5}$ mass concentrations were higher than the PM_{10} mass concentrations. For this reason, an additional measuring device of which measuring procedures for $PM_{2.5}$ and PM_{10} are completely consistent was utilized to correct original data. Firstly, the ratio of $PM_{2.5}$ and PM_{10} concentrations provided by the additional device was calculated with respect to time. Using this ratio, the original PM_{10} measurements were corrected. Data obtained from the additional device were not available after 18 February. Consequently, a constant, based on the existing measuring data and other research results[29-31], was used to correct remaining data. The data of 1st February to 18th February were corrected by different factors per hour. The values fluctuated from 1.1(1/0.9) to 1.4(1/0.7).The rest data were corrected by an average value of 1.3(1/0.77).

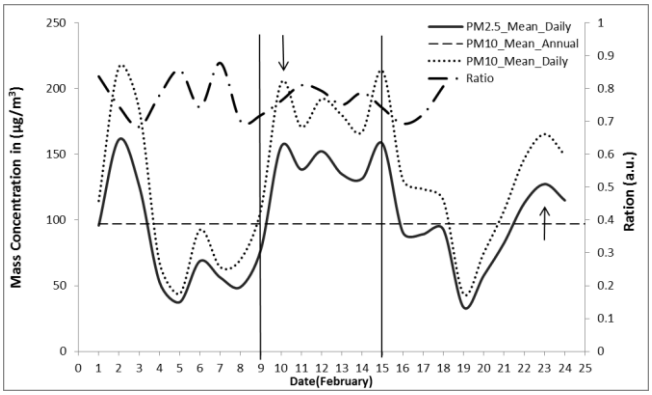

Figure 2 Daily mean mass concentrations of $PM_{2.5}$ and PM_{10} during spring festival

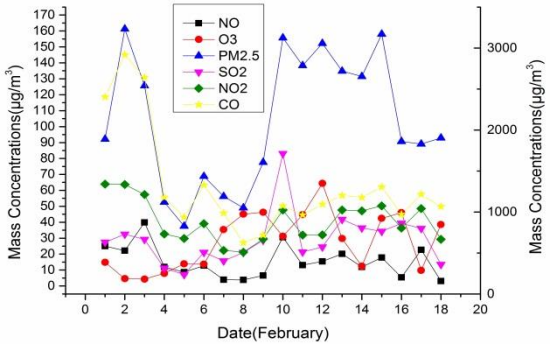

Figure 3 Daily mean mass concentrations of gaseous pollutants.

Seasonal differences in particulate matter mass concentrations were evident in our study area over the observation years, but were irrelevant factors and not included in this study. For this reason, only February 2013 data are presented. The 2012 annual mean PM_{10} mass concentration was released by the Wuhan Environmental Protection Bureau. However, there was no annual mean $PM_{2.5}$ concentration, because 2013 was the first year that $PM_{2.5}$ was monitored and published by the government of China. The down arrow in Fig. 2 denotes the first day of the lunar new year and the up arrow denotes the fifteenth day of the lunar new year, namely lantern day. Two vertical lines denote the seven-day public holiday. The original data were converted to a daily time scale by averaging 24 hourly measurements per day.

Figure 2 shows that concentrations of both $PM_{2.5}$ and PM_{10} rose dramatically on NYE and remained high during the public holiday. However, concentrations of $PM_{2.5}$ and PM_{10} rose slightly on lantern day indicating NYE is a more valuable period for studying celebration effects. Besides, an increase is also observed on the 2nd of February. Figure 3 shows that CO, NO and NO2 concentrations were abnormal on the 2nd February. Among them, the CO concentration was incredibly high. In the Figure 3,CO marks the right axis while other pollutants share the left one. Considering that 2nd February was the last public holiday before the Spring Festival. People rushed out to prepare food and goods for the Spring Festival on this day. Vehicle emission may be responsible for the increase of PM2.5/10 on this day.

The ratio of $PM_{2.5}$ and PM_{10} fluctuated, but no trend was evident on NYE, indicating that firecracker influences on $PM_{2.5}$ and PM_{10} may be homogeneous. Thus, we speculate firecracker activities do not exert influences on particulate matter size distribution.

Figure 2 and Figure 3 suggest a daily study of firecracker influences may be an unsuitable time scale, since the highest daily concentrations of $PM_{2.5}$ and PM_{10} appeared on 2nd February when firecracker activities were forbidden. So in the following sections, the hourly mean concentration was utilized to reveal firecracker effects on ambient air quality.

Besides, $PM_{2.5}$ is believed to be a greater health threat than PM_{10} since the smaller particles are more likely to be deposited deep into lungs. Moreover, $PM_{2.5}$ concentration has become controversial in Chinese public opinion since serious smog frequently envelops most Chinese cities. Consequently, a more detailed study solely focused on $PM_{2.5}$ was necessary.

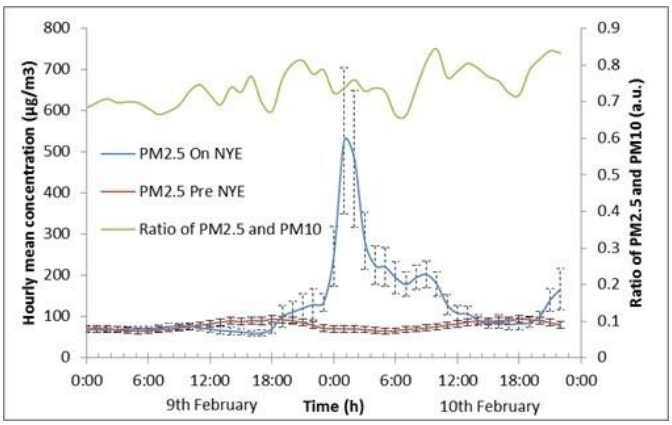

Figure 4 Hourly mean mass concentrations of $PM_{2.5}$

As data were collected from ten different sites, averages and variances were calculated and are presented in Fig. 4. The error bars represent variances of data measured at different sites. The green line represents the hourly ratio of $PM_{2.5}$ and PM_{10}.

On normal days, the $PM_{2.5}$ concentrations remained around 80 $\mu g/m^3$ and consistent throughout the day. Meanwhile, we found a homogeneous distribution of $PM_{2.5}$ concentrations due to minimal, yet consistent variance. Before 20:00 on NYE, $PM_{2.5}$ concentrations were similar to normal days. According to tradition, 0:00 on the first day of the lunar New Year was when people spontaneously, and intensely, ignited firecrackers. Celebrations often ended within an hour because people went to sleep. The hourly mean $PM_{2.5}$ concentrations rose rapidly after 0:00 on 10 February. The highest $PM_{2.5}$ concentration of 526.5$\mu g/m^3$ occurred at 1:00 on 10 February, nearly seven-fold background values. $PM_{2.5}$ concentration remained high until 12:00 on 10 February. We conclude the influence of firecracker activities on $PM_{2.5}$ concentrations was instant, evident, and durable.

A similar trend between variances and averages was found. Variance increased to 355.3$\mu g/m^3$ at 1:00 on 10 February, 23

times background values, indicating a heterogeneous distribution of $PM_{2.5}$ concentrations after firecracker activities. We conclude firecrackers burning not only increased the $PM_{2.5}$ concentrations, but also changed its distribution. $PM_{2.5}$ distribution differences and the key factor behind such phenomenon are discussed further below.

Finally, the ratio of $PM_{2.5}$ and PM_{10} revealed no temporal trend even after a finer resolution was adopted. This supports our conclusion that firecrackers burning would not influence the size distribution of atmospheric particulate matter.

Spatial distribution of $PM_{2.5}$ emitted by firecracker activities

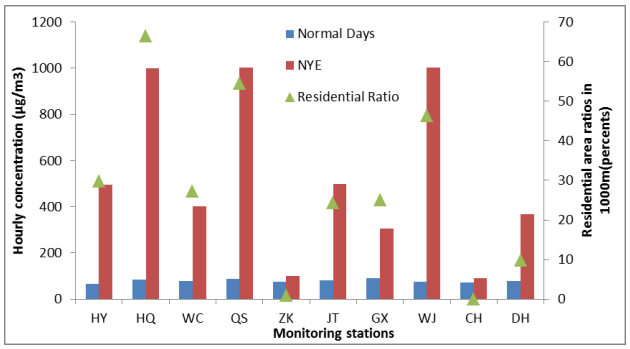

Figure 5 Comparison of $PM_{2.5}$ distributions on normal days and NYE

The blue columns in Fig. 5 represent average hourly $PM_{2.5}$ mass concentrations based on data observed before 11:00 on 9 February. Red columns represent hourly concentrations observed at 1:00 on 10 February, coincident with major firecrackers activities. As described above, ten monitoring sites were distributed across different parts of the city. Some were located in residential areas and others were near industry or businesses. One site is far away from the urban centre. However, Fig. 5 illustrates the homogeneous spatial distribution of PM2.5 on non-celebration days in Wuhan. In contrast, a heterogeneous distribution is evident during NYE. $PM_{2.5}$ concentrations measured at CH and ZK during NYE were slightly higher than non-celebration days, showing these two sites are partially free from the influence of firecrackers. Hourly $PM_{2.5}$ mass concentration rose dramatically at HQ, QS, and WJ and increased in varying amounts at other sites. From the perspective of information theory, high variances suggest more information. Hence,there must be some factors that brought new information and changed the pristine distribution pattern.

A striking feature of Chinese NYE celebrations is the spontaneous and unorganized burning of firecrackers and fireworks, and is distinct from other fireworks displays described in previous studies[6, 11, 12, 14, 27]. So the pollutant sources should be regarded as several planes, but not singular points. Two key factors determine pollutant emissions. One is the population in a certain area and the other is per capita emissions. It was presumed that pollution levels mirror population. As it is practically impossible to count citizens in certain areas, a linear relationship between the population and the size of residential areas was assumed, since people often ignite firecrackers just outside their houses on NYE. In addition, WJ data were excluded when establishing the regression equation, because we felt the per capita emission in this area was clearly more than other sites. WJ was located in a newly developed urban area, recently transformed from rural area. According to our knowledge, and Chinese tradition, the per capita $PM_{2.5}$ firecrackers activities emission in rural areas always significantly exceeds urban areas. Data in Fig. 5 supports this assumption. To establish a single equation, a weighting function was required when both rural and urban areas were included. Unfortunately, we have no quantitative weighting function to describe differences in per capita emissions, so accuracy of our regression model required the exclusion of WJ data.

On that basis, a relationship between $PM_{2.5}$ concentration and residential area was established and is shown in Fig. 6. Residential area ratios were calculated first by dividing total area by residential area. We tested the proper way to determine the radius of the total area, evaluating at both 500 m and 1000 m. Larger radii were not tested because they were too far away from monitoring stations to reflect the real-time situation of ambient air. A radius of 1000 m proved to be the best.

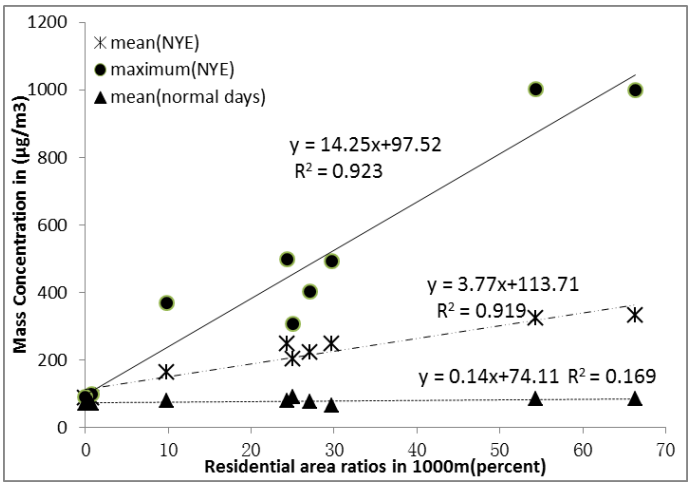

Figure 6 Relationship between $PM_{2.5}$ concentration and residential area ratios

The circles in Fig. 6 denote $PM_{2.5}$ concentrations measured at nine sites at 1:00 on 10 February. These values were the maximums for most monitoring sites throughout the entire monitoring period, except CH and ZK. An asterisk denotes mean $PM_{2.5}$ concentration on NYE, based on original data measured from 20:00 on 9 February to 8:00 on 10 February. A triangle denotes mean $PM_{2.5}$ concentrations measured at each site during the pre-celebration period from 1-9 February. Minor differences in $PM_{2.5}$ concentrations measured at different sites on non-celebration days indicated little relation between residential area and $PM_{2.5}$ concentration. However, a significant relationship exists between those two factors on NYE. Data in Fig. 6 show either R^2 value of these corresponding regressions exceed 0.91. Hence, both maximum hourly concentration and average daily concentration can be estimated using residential

data. These equations also explain why variances of $PM_{2.5}$ concentrations measured at different sites on NYE yet remained low on days, as shown in Fig. 4.

We conclude estimations of contaminants due to NYE celebrations in urban areas can be calculated using urban planning data along with our equations. Remote sensed images can be used to fulfil this need. Residential information can be extracted from remote sensed images using well-developed methods, such as supervised classification or artificial interpretation.

Vertical and temporal distribution of $PM_{2.5}$ emitted by firecracker activities

Correlations of Ceilometer backscatter with PM_{10} in Hanover was reported by Münkel[32]. We expected Lidar observations could help reveal the vertical distribution of suspended particulate matter generated by human-induced perturbations. We demonstrated NYE celebrations generated lots of contaminants causing a dramatic rise in $PM_{2.5}$ concentrations. There is a known negative correlation between $PM_{2.5}$ concentrations and visibilities. Hence, we retrieved aerosol extinction coefficients based on observations of our Mie Lidar using the classic inversion algorithm proposed by Fernald (Fernald 1984), aiming at reflecting contaminant vertical distributions.

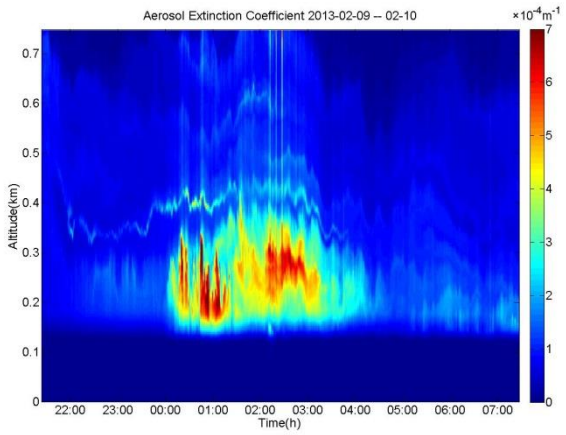

Figure 7 Variations of atmospheric extinction coefficients on the NYE.

Figure 7 illustrates aerosol extinction coefficients measured from 22:00 on 9 February to 7:00 on 10 February. Because the major celebration activities began at 0:00 on 10 February and ended no more than 1 hour later, the ultimate temporal resolution of our Lidar data was one second. However, such high temporal resolution was unnecessary for this study. When the frequency of a Lidar is fixed, long averaging time means a larger signal-to-noise ratio (SNR). Hence, we selected a one minute time interval to balance temporal resolution and reliability of the data.

In Fig. 7, it is incorrect to conclude the air near the ground is very clean from the illusion that the atmospheric extinction coefficients measured under 180 m are nearly zero. Actually, this phenomenon is due to the so-called overlap factor. The overlap factor (i.e. the crossover, geometrical compression or geometrical form factor) is an effect of reduced detection or response to the Lidar return signal caused by the misalignment of transmitter– receiver systems and the inaccuracy attributed to the optical device of receiver systems. According to our previous study, the relative error of the overlap factor are minimized at altitudes above 200 meters[33]. This explains why extinction coefficients of less than 180 m in Fig. 7 were obviously unrealistic. Moreover, the reference datum of "altitude" used here is the height of the roof of our laboratory, about 15 meters from the ground. Unlike other fireworks displays of celebrations around the world, the major pollution sources on NYE were firecrackers set off on the ground, not the fireworks plume emitted in the air. Therefore, we believe concentrations of particulate matter at low altitudes (below 200 m) exceeded those at high altitudes and similar trends for extinction coefficients.

We found a few people ignited fireworks and firecrackers in a small square 200 m from our Lidar at 22:00, as shown in Fig. 7 as a small rise in extinction coefficients at about the same time, indicating that even sporadic fireworks and firecrackers activities may affect atmospheric aerosol optical properties. Dramatic change in aerosol extinction coefficients appeared at 0:00 on 10 February coincident with the start of traditional NYE celebrations. Moreover, the effect of fireworks and firecrackers activities on atmospheric aerosol did not fade away until altitudes greater than 400 m, and almost disappeared above 500 m. For this reason, the maximum range of Fig. 7 is 750 m, in spite of maximum detection ranges of 15 km. Retrievals of altitudes above 5 km were inaccurate from 0:00 to 4:00 on 10 February because of a dramatic drop in laser energy. The laser cannot fully penetrate the atmosphere beyond 750 m under these circumstances, and the upper atmospheric composition is imprecise. Such phenomenon implied the tremendous changes of atmospheric aerosol optical properties at low altitude were caused by the burning of firecrackers and fireworks. Figure 7 also shows the vertical diffusion process of contaminants due to celebration activities. The extinction coefficients of the upper atmosphere measured right after 0:00 were less than later measurements. The affected altitude increased from less than 300 m to over 450 m over time. Contaminants reached maximum vertical influence area two hours after the celebration activities ceased, as shown in Fig. 7. The vertical influence began to fade away after 2:00, implying dry deposition then became the dominant factor.

Aerosol extinction coefficients did not return to pre-celebration level even at 7:00 on 10 February. Figure 7 shows the duration of significant atmospheric influences 150 m above the ground was about 4.5 hours in the light. Such duration was much longer than that reported in E. A. Vallar, R. Calhoun and van der Kamp[25-27], showing a grander scale of celebrations happened on NYE.

$PM_{2.5}$ data were also used to reflect the temporal variations of contaminants due to celebration activities. CH and ZK data were used as background. GX, WC, HQ, QS, and HY were

selected as representatives of urban areas. The proximity of monitoring sites to firecrackers activities was our major concern in selecting urban representatives. Uniformities of geographical distribution and data quality were also considerations. In Fig. 8, the black line reflects average hourly $PM_{2.5}$ mass concentrations measured at the five urban sites. The red and blue lines, sharing the right vertical axis, denote background data collected from CH and ZK, respectively.

The hourly $PM_{2.5}$ mass concentrations of urban sites reached their maximum at 1:00 on 10 February, coincident with major celebration activities. The $PM_{2.5}$ concentrations remained high over the next hour and then decreased sharply after 2:00. Five hours later concentrations returned below $200\mu g/m^3$, indicating significant influences had already faded away. In view of concentrations measured before celebrations, namely around $70\mu g/m^3$, we conclude the influence of celebration activities vanished 15 hours after celebrations ceased. Several relatively smaller peaks emerged in later days, probably due to smaller scale celebrations usually at dinner time, particularly in the following five to six days.

Two background sites showed different temporal variation patterns in $PM_{2.5}$. Figure 8 shows the first peak of ZK curve emerged at 2:00 on NYE, one hour later than urban sites, undergoing dispersion of contaminants. Unlike the urban curve, double peaks were observed in the ZK curve. We believe the first peak was due to celebration activities within the residential area near the monitoring station, and the second one may be due to dispersion of contaminants from the more populated Hanyang district about 10 km away. Figure 8 also shows small celebrations play a more important role in rural area air pollution than that of urban areas, because the highest $PM_{2.5}$ concentrations at CH site appeared two days later.

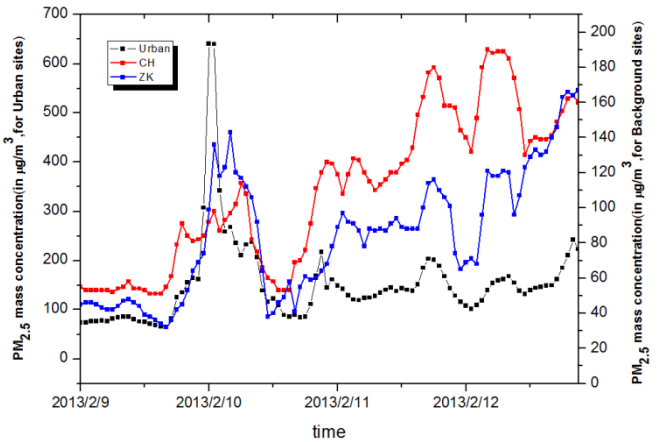

Figure 8 Different temporal variations of $PM_{2.5}$ between urban and nonresidential area.

Estimation of PM2.5 Emissions from Celebration Activities on the NYE

To estimate the $PM_{2.5}$ emissions from fireworks and firecrackers activities on NYE in Wuhan, the non-celebrations $PM_{2.5}$ mass concentration (assuming there were no celebrations-induced perturbations), was simulated using the two models of totally distinct core ideas. Using data measured at CH and ZK as references, we established relationships between $PM_{2.5}$ mass concentrations of residential areas and non-residential areas. Based on the analysis above, we assumed the influence of NYE celebrations on $PM_{2.5}$ mass concentration was negligible for monitoring stations located far from residential areas. The mean non-celebration $PM_{2.5}$ mass concentration of urban area was then simulated by building a regression analysis model using input measurements acquired at CH and ZK. We used time series analysis[34] to estimate non-celebrations $PM_{2.5}$ mass concentration. Measurements from ten sites taken before 18:00 on 9 February were used to build the model, and we then simulated concentrations for the time period of 19:00 on 9 February to 9:00 on 10 February.

Simulated and measured values are shown in Fig. 9. ZK and CH measurements were excluded because these sites are not in urban areas. The standard deviation of the estimate, $15.40\mu g/m^3$, was adopted as a precision evaluation index for our regression model. Because there was no such index for time series analysis, another eight simulations were calculated to evaluate precision after comparison with actual measurements. The mean absolute error (MAE), $18.75\mu g/m^3$, was n calculated as a precision evaluation index for this model. MAE was calculated in equation 1 below. C_m was the measuring concentration and C_s was the simulation.

$$\mathrm{MAE} = \overline{|C_m - C_s|} \quad (1)$$

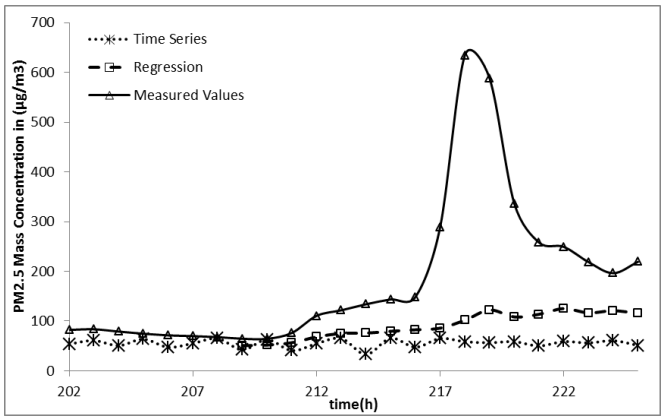

Figure 9 Simulations and measurements of $PM_{2.5}$ on the NYE.

Profiles of aerosol extinction coefficients were used to describe the vertical distribution of $PM_{2.5}$ and residential area of Wuhan was 500 km^2, according to government data.

$$\mathrm{M} = \int_0^Z S(\overline{C_m} - \overline{C_s})D(z)dz \quad (2)$$

Estimation of $PM_{2.5}$ emissions from fireworks and firecrackers activities was calculated in equation (2). M was the total mass, S was the area of settlement places D(z) was the vertical distribution, $\overline{C_m}$ was the average of maximum $PM_{2.5}$ mass concentrations measured by eight sites distributed around urban area, and $\overline{C_s}$ was the corresponding simulation. Based on our

calculations, the total mass of $PM_{2.5}$ emissions in Wuhan on NYE were 39.57 (Regression) and 43.51 (time series) tons.

Conclusions

A Mie Lidar and ten air quality monitoring stations distributed across the city of Wuhan were utilized to study the spatial, vertical, and temporal distributions and variations of human-induced contaminations due to Chinese NYE celebrations. We found dramatic changes in aerosol particle concentrations on NYE in Wuhan. The highest average of hourly $PM_{2.5}$ concentrations, measured at ten monitoring stations, was 526.5μg/m^3 with standard deviation of 355.3μg/m^3; this is 7 times larger than concentrations measured on ordinary days. No change in the ratio of $PM_{2.5}$ and PM_{10} was observed, implying that the influence of the firecracker activities on the concentration of particulate matter is not selective. A significant linear correlation between $PM_{2.5}$ concentration and residential area in urban areas was found, which may be useful to evaluate future pollutant distributions from similar annual celebrations in China. Moreover, we determined the vertical distribution of contaminants emitted by the burning of fireworks and firecrackers on NYE for the first time. We found that the influences of firecracker activities on the atmosphere existed for altitudes up to 500 m, and such influences lasted for over 4 hours. Contaminations spread from the ground to over 300 m in altitude immediately after the celebrations started and lingered 200–350 m above the ground for a long time before dry deposition. Influences vanished 15 hours after the major firecracker activities ended. Finally, we estimated that 39.57–43.51 tons $PM_{2.5}$ was emitted in February 2013 by human-induced activities around the whole city, according to two different models.

Acknowledgements

This research was supported by the National Nature Science Foundation of China（NFFC）No. 41127901. We are also sincerely thankful for constructive comments from the anonymous reviewers.

1. A. Henneberger, W. Zareba, A. Ibald-Mulli, R. Rückerl, J. Cyrys, J.-P. Couderc, B. Mykins, G. Woelke, H.-E. Wichmann and A. Peters, *Environmental health perspectives*, 2005, 113, 440.
2. A. Peters, D. W. Dockery, J. E. Muller and M. A. Mittleman, *Circulation*, 2001, 103, 2810-2815.
3. D. R. Gold, A. Litonjua, J. Schwartz, E. Lovett, A. Larson, B. Nearing, G. Allen, M. Verrier, R. Cherry and R. Verrier, *Circulation*, 2000, 101, 1267-1273.
4. K. Ravindra, S. Mor and C. P. Kaushik, *Journal of Environmental Monitoring*, 2003, 5, 260-264.
5. I. van Kamp, P. G. van der Velden, R. K. Stellato, J. Roorda, J. Loon, R. J. Kleber, B. B. R. Gersons and E. Lebret, *European Journal of Public Health*, 2006, 16, 252-258.
6. S. Tiwari, D. M. Chate, M. K. Srivastava, P. D. Safai, A. K. Srivastava, D. S. Bisht and B. Padmanabhamurty, *Natural Hazards*, 2012, 61, 521-531.
7. S. C. Barman, R. Singh, M. P. S. Negi and S. K. Bhargava, *Journal of Environmental Biology*, 2009, 30, 625-632.
8. P. S. Rao, D. G. Gajghate, A. G. Gavane, P. Suryawanshi, C. Chauhan, S. Mishra, N. Gupta, C. V. C. Rao and S. R. Wate, *Bulletin of Environmental Contamination and Toxicology*, 2012, 89, 376-379.
9. S. Sarkar, P. S. Khillare, D. S. Jyethi, A. Hasan and M. Parween, *Journal of Hazardous Materials*, 2010, 184, 321-330.
10. T. Moreno, X. Querol, A. Alastuey, F. Amato, J. Pey, M. Pandolfi, N. Kuenzli, L. Bouso, M. Rivera and W. Gibbons, *Journal of Hazardous Materials*, 2010, 183, 945-949.
11. T. Moreno, X. Querol, A. Alastuey, M. C. Minguillon, J. Pey, S. Rodriguez, J. V. Miro, C. Felis and W. Gibbons, *Atmospheric Environment*, 2007, 41, 913-922.
12. R. Vecchi, V. Bernardoni, D. Cricchio, A. D'Alessandro, P. Fermo, F. Lucarelli, S. Nava, A. Plazzalunga and G. Valli, *Atmospheric Environment*, 2008, 42, 1121-1132.
13. F. Drewnick, S. S. Hings, J. Curtius, G. Eerdekens and J. Williams, *Atmospheric Environment*, 2006, 40, 4316-4327.
14. H. H. Tsai, L. H. Chien, C. S. Yuan, Y. C. Lin, Y. H. Jen and I. R. Ie, *Atmospheric Environment*, 2012, 62, 256-264.
15. S. C. Chang, T. H. Lin, C. Y. Young and C. T. Lee, *Environmental Monitoring and Assessment*, 2011, 172, 463-479.
16. T. M. Do, C. F. Wang, Y. K. Hsieh and H. F. Hsieh, *Aerosol and Air Quality Research*, 2012, 12, 981-993.
17. Y. Wang, G. S. Zhuang, C. Xu and Z. S. An, *Atmospheric Environment*, 2007, 41, 417-431.
18. M. Zhang, X. M. Wang, J. M. Chen, T. T. Cheng, T. Wang, X. Yang, Y. G. Gong, F. H. Geng and C. H. Chen, *Atmospheric Environment*, 2010, 44, 5191-5198.
19. J. L. Feng, P. Sun, X. L. Hu, W. Zhao, M. H. Wu and J. M. Fu, *Atmospheric Research*, 2012, 118, 435-444.
20. W. Gong, J. Zhang, F. Mao and J. Li, *Chinese Optics Letters*, 2010, 8, 533-536.
21. MEP, 2012, vol. GB 3095-2012.
22. CMA, 2007, vol. QX/T 51-2007.
23. CMA, 2007, vol. QX/T 50-2007.
24. CMA, 2007, vol. QX/T 49-2007.
25. E. A. Vallar, M. C. D. Galvez, J. C. Q. Uy, E. P. Macalalad, T. A. Roman and E. B. Bangsal, in *22nd International Laser Radar Conference*, eds. G. Pappalardo and A. Amodeo, 2004, vol. 561, pp. 549-552.
26. R. Calhoun, R. Heap, J. Sommer, M. Princevac, J. Peccia and H. Fernando, in *Sensors, and Command, Control, Communications, and Intelligence(C31) Technologies for Homeland Security and Homeland Defense Iii, Pts 1 and 2*, ed. E. M. Carapezza, 2004, vol. 5403, pp. 683-694.
27. D. van der Kamp, I. McKendry, M. Wong and R. Stull, *Atmospheric Environment*, 2008, 42, 7174-7178.
28. S. S. Lim, T. Vos, A. D. Flaxman, G. Danaei, K. Shibuya, H. Adair-Rohani, M. Amann, H. R. Anderson, K. G. Andrews and M. Aryee, *The Lancet*, 2013, 380, 2224-2260.
29. J. R. Brook, T. F. Dann and R. T. Burnett, *Journal of the Air & Waste Management Association*, 1997, 47, 2-19.

30. W. F. McDonnell, N. Nishino-Ishikawa, F. F. Petersen, L. H. Chen and D. E. Abbey, *Journal of exposure analysis and environmental epidemiology*, 2000, 10, 427-436.
31. X. Querol, A. Alastuey, M. M. Viana, S. Rodriguez, B. Artiñano, P. Salvador, S. Garcia do Santos, R. Fernandez Patier, C. R. Ruiz, J. de la Rosa, A. Sanchez de la Campa, M. Menendez and J. I. Gil, *Journal of Aerosol Science*, 2004, 35, 1151-1172.
32. C. Münkel, N. Eresmaa, J. Räsänen and A. Karppinen, *Boundary-layer meteorology*, 2007, 124, 117-128.
33. W. Gong, F. Mao and J. Li, *Optics Communications*, 2011, 284, 2966-2971.
34. J. D. Hamilton, *Time series analysis*, Cambridge Univ Press, 1994.